Article

Network Homeostasis and State Dynamics of Neocortical Sleep

Highlights

- Pyramidal cell firing rates are widely distributed and skewed toward high firing rates

- Neurons from opposite ends of that distribution are oppositely modulated by sleep

- Sleep stages have systematically varying effects on neurons of different firing rates

- REM, nonREM, and microarousal effects cooperate to create the sleep homeostatic effect

Authors

Brendon O. Watson, Daniel Levenstein, J. Palmer Greene, Jennifer N. Gelinas, György Buzsáki

Correspondence

gyorgy.buzsaki@nyumc.org

In Brief

Watson et al. reveal a new form of regulation of neural activity by sleep. The firing rates of fast- and slow-firing neurons are homogenized over sleep. This effect is due to contributions from REM, nonREM, and sleep microarousals.

CrossMark

CellPress

Network Homeostasis and State Dynamics of Neocortical Sleep

Brendon O. Watson,[1,3] Daniel Levenstein,[1,2] J. Palmer Greene,[1] Jennifer N. Gelinas,[1] and György Buzsáki[1,2,*]
[1]New York University Neuroscience Institute
[2]Center for Neural Science
New York University, New York, NY 10016, USA
[3]Department of Psychiatry, Weill Cornell Medical College, New York, NY 10065, USA
*Correspondence: gyorgy.buzsaki@nyumc.org
http://dx.doi.org/10.1016/j.neuron.2016.03.036

SUMMARY

Sleep exerts many effects on mammalian forebrain networks, including homeostatic effects on both synaptic strengths and firing rates. We used large-scale recordings to examine the activity of neurons in the frontal cortex of rats and first observed that the distribution of pyramidal cell firing rates was wide and strongly skewed toward high firing rates. Moreover, neurons from different parts of that distribution were differentially modulated by sleep substates. Periods of nonREM sleep reduced the activity of high firing rate neurons and tended to upregulate firing of slow-firing neurons. By contrast, the effect of REM was to reduce firing rates across the entire rate spectrum. Microarousals, interspersed within nonREM epochs, increased firing rates of slow-firing neurons. The net result of sleep was to homogenize the firing rate distribution. These findings are at variance with current homeostatic models and provide a novel view of sleep in adjusting network excitability.

INTRODUCTION

Sleep exerts profound effects on brain and body, including regulation of the endocrine (Rasch and Born, 2013) and immune systems (Besedovsky et al., 2012), extracellular clearance of potentially toxic substances (Xie et al., 2013), recovery from brain damage (Siccoli et al., 2008), construction of circuits during development (Frank et al., 2001), and consolidation of learned information (Axmacher et al., 2006; Buzsáki, 2015; Inostroza and Born, 2013; Rasch and Born, 2013; Sejnowski and Destexhe, 2000).

Mounting evidence is available to support a homeostatic role for sleep, particularly for the importance of non-rapid eye movement (nonREM) sleep (Borbély, 1982; Feinberg, 1974; Tononi and Cirelli, 2003, 2014). An influential model, the synaptic homeostasis hypothesis (SHY), suggests that a major role for sleep is to facilitate recuperation of neuronal energy and synaptic resources that have been depleted after prolonged waking (Tononi and Cirelli, 2003, 2014). A prediction of SHY is that the most active cells and synapses during waking continue to be active during sleep, whereas weak synapses and slow-firing neurons are "down-selected," that is, eliminated from network activity (Tononi and Cirelli, 2003; Vyazovskiy and Harris, 2013). Another homeostatic scaling model assumes a uniform synaptic and rate adjustment by multiplying or dividing each synaptic strength and rate by a uniform factor (Turrigiano and Nelson, 2004; Turrigiano et al., 1998). However, these key predictions of the SHY and synaptic homeostatic scaling models have not been tested during natural sleep.

In support of the synapse-oriented predictions of SHY, firing rates of neocortical and hippocampal principal neurons have been found to generally increase during waking and decrease over sleep in rats (Grosmark et al., 2012; Miyawaki and Diba, 2016; Mizuseki and Buzsáki, 2013; Vyazovskiy et al., 2009), and the amplitude of evoked responses has been found to vary as a function of sleep-wake cycle (Vyazovskiy et al., 2007). However, even neurons of similar nominal classification vary greatly and may be regulated differentially. Pyramidal neurons show a range of synaptic weights and firing rates that vary over several orders of magnitude (Buzsáki and Mizuseki, 2014). The distribution of these variables over the population is not just broad but also highly skewed, and approximates a lognormal distribution. These observations suggest that the contributions of neurons at high and low ends of the firing rate spectrum are systematically organized and differentiated (Lim et al., 2015; Mizuseki and Buzsáki, 2013). Therefore, whether sleep affects neurons from different ends of this distribution uniformly remains an open question with important functional implications.

Furthermore, it remains to be understood how the evolutionarily conserved nonREM and REM states differentially contribute to homeostasis (Gervasoni et al., 2004; McCarley, 2007). Recent work has shown that REM can decrease firing rates in the hippocampus (Grosmark et al., 2012), which is of particular interest when combined with findings that REM and nonREM sleep may contribute to different types of memory (Grosmark and Buzsáki, 2016; Rasch and Born, 2013) and that alterations of REM sleep can affect cognitive and affective disorders (Gierz et al., 1987; Walker, 2010). Furthermore, there is evidence from humans that relative abundance of REM and nonREM plays a role in learning (Stickgold et al., 2000), but whether these substates of sleep play distinct roles in homeostasis is not known.

In this study, we sought to understand the homeostatic regulation of cortical neurons from across the spectrum of firing rates

and how sleep substates differentially contribute to that process. First, we find that fast-firing pyramidal neurons decrease their firing over sleep, whereas slow-firing neurons increase their rates, resulting in a narrower population firing rate distribution after sleep. Second, each sleep substate makes a unique contribution to this overall renormalization process. Our findings reveal a novel form of homeostasis in the brain: regulation of the variance of the system as a focal process in maintaining network balance.

RESULTS

To examine how different aspects of sleep affect firing patterns of neurons, we automatically classified brain states, categorized neurons based on their activity during waking (WAKE), and tracked them individually during various stages of sleep. We then assessed (1) differences in average neuronal firing metrics in sleep states, (2) progressive spiking and local field potential (LFP) changes over the course of those sleep states, and (3) how within-state firing rate changes persisted into subsequent states.

Identification of Brain States
We recorded across different brain states from 11 rats implanted with one or two 64-site silicon probes in frontal cortical areas, including the medial prefrontal cortex, orbitofrontal cortex, anterior cingulate cortex, and secondary motor cortex (Figure S1A, available online). Recordings from 27 sessions (294 ± 137 min) during the light cycle were segregated into WAKE, nonREM, REM episodes, and microarousals (MAs; Figure 1; Table S1). Brain state segregation was performed by a heuristic automated approach and verified by independent visual classification (Figures 1A–1D and S1C). First, LFPs were converted into spectrograms and principal component analysis was performed on each spectrogram. In all recordings, the first principal component (PC1) was found to represent power in the low-frequency ranges, with weights of frequencies <25 Hz opposite in sign to those of frequencies in the gamma range. Since the magnitude of PC1 showed a bimodal distribution (Figure 1C), a threshold was set at the trough between the two peaks of the distribution, which allowed us to classify each second as either nonREM (high PC1 power) or "other" state (low PC1 power). The next step classified the "other" epochs using a narrow band theta power ratio (5–10 Hz/2–16 Hz) and electromyogram (EMG) measures (Figures 1C and S1C), also using cutoffs at the minima of bimodal distributions on a per recording session basis. Before proceeding, epochs with high theta power and low EMG activity were designated as REM.

The remaining "arousal" epochs were divided into two further groups. Prolonged epochs, which often resulted in overt movement (mean epoch movement >5 SD of nonREM mean movement), high EMG activity, and high theta power, were called WAKE. Shorter epochs (<40 s; Figure S1D), characterized by low theta power but elevated EMG compared to REM or nonREM (Figures 1A and 1B), were typically embedded between nonREM epochs. Our 40 s cutoff was based on the statistical observation that this threshold yielded MA epochs without consistent movement (Figure S1D). Previous work has referred to such patterns as "low-amplitude sleep" (Bergmann et al.,

1987), "low-amplitude irregular activity" (Pickenhain and Klingberg, 1967), or MAs (Halász et al., 1979; Schieber et al., 1971). We refer to them here as MAs and restricted our classification of these states to only those which occur between nonREM periods. There were a total of 790 MAs in our dataset (median duration = 15.9 ± 3.3 s; frequency = 0.32 ± 0.12 per minute; 9.1% ± 3.5% of time in SLEEP [a time epoch defined in detail below]). Over nonREM episodes, the fraction of time occupied by MAs decreased (correlation versus normalized nonREM episode time was as follows: R = −0.85, p < 10^{-10}), with no statistical change over the course of SLEEP.

Uninterrupted nonREM epochs are referred to here as nonREM "packets," whereas a stream of nonREM packets and MAs without REM are called "nonREM episodes" (Figure 1A; definitions in Table S1). We found that the duration of packets was distributed over two orders of magnitude, with a median of 111 s. Alternating nonREM and REM episodes, lasting a minimum of 20 min and terminated by prolonged (>120 s) WAKE are termed extended SLEEP session (Figure 1A). Finally, we designated analyzable WAKE-SLEEP cycles using cutoffs of a ≥7 min WAKE period followed by a ≥20 min SLEEP period. The wake cutoff of 7 min was chosen because it met the intuitive criterion of yielding WAKE epochs highly correlated with ambulation.

In addition to these longer timescale states, we detected ~0.1–4 s long UP and DOWN states (Wilson and Groves, 1981), which respectively represent two poles of a bimodal but irregular pattern of population firing during nonREM sleep (Steriade, 2006). DOWN states were characterized by lack of neuronal spiking activity, prominent delta waves, and reduced gamma-band power. UP states were detected as events with spiking activity following clear DOWN states (details of detection algorithm in Supplemental Information). Within UP states, we were able to characterize the evolution of LFP (Figure 1E, upper part), as well as spiking metrics, including rates of spiking (Figure 1E, lower part) of putative pyramidal or excitatory (pE) and putative inhibitory (pI) units (unit classification in Figure S2A).

Assessment of Firing Patterns in Different Brain States
Neuronal spiking was recorded from deep cortical layers (Figure S1A), identified by the positive polarity of DOWN states in the LFP (Buzsáki et al., 1988; Calvet et al., 1973). Criteria for clustering of single units and separation of principal neurons from interneurons have been described in detail previously (Supplemental Information). Neurons that did not meet the strict criteria for clean clusters and recording stability (Schmitzer-Torbert et al., 2005) were discarded. Sessions without full WAKE-SLEEP cycles (Supplemental Information) were also discarded. This resulted in 995 putative pyramidal cells (pE; mean of 36.9 cells/session; range of 10–104) and 126 putative interneurons (pI; 4.67 cells/session; range of 0–13). Statistics were carried out on a per-cell basis and only on putative pyramidal neurons, unless otherwise specified.

Neuronal firing varied according to brain state. Across all states, the distribution of per-cell mean firing rates for putative pyramidal neurons was strongly positively skewed, with a log-normal tail toward higher frequencies and a supra-log-normal tail toward lower frequencies (Figure S2C), spanning three
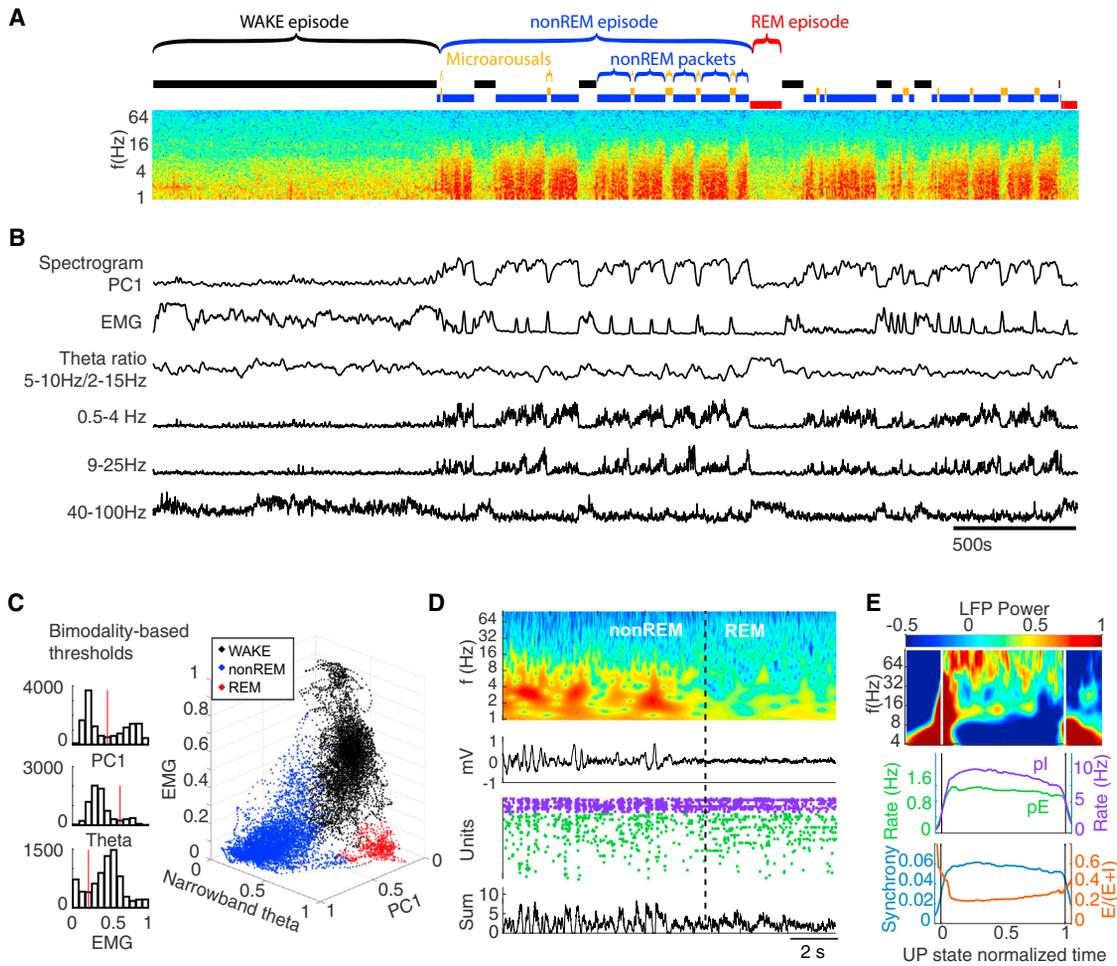
Figure 1. Classification of Brain States

(A) Time-power analysis of cortical local field potentials (LFPs). Time-resolved fast Fourier transform-based power spectrum of the LFP recorded from one site of a 64-site silicon probe in layer 5 of the orbitofrontal cortex. Epochs generated by manually approved automatic brain state segregation are shown above the spectrum.

(B) Metrics extracted for state classification. The first principal component (PC1) of the LFP spectrogram segregated nonREM packets from "other" epochs. Non-nonREM epochs with high theta power and low electromyogram (EMG) activity were designated as REM. Remaining epochs were termed either as WAKE (>40 s) or microarousal (MA; <40 s; see Figure S1D and Results). Alternating epochs of nonREM packets and MAs comprise nonREM episodes. Integrated power in the delta (0.5–4 Hz), sigma (9–25 Hz) and gamma (40–100 Hz) bands over time is also shown.

(C) State separation. Left: bimodal distributions and threshold values (red vertical lines) of PC1, theta power, and EMG, respectively. These were used for state segregation in the example session in (A). Right: three-dimensional plot showing the automatic state segregation. Each point corresponds to 1 s of recording time, with color indicating the identified state during that second as labeled.

(D) Example state transition. Top two panels show time-resolved wavelet power spectrum and corresponding raw LFP across a nonREM-REM state transition. Concurrent spikes of putative interneurons (purple dots) and pyramidal cells (green) are shown. Below: summed spikes of all pyramidal cells. Note correspondence between silent periods of spike rasters (DOWN state) and large positive waves in the LFP. This change between intermittent activity and persistent activity differentiates nonREM from REM in the cortex and is also represented in PC1 of the LFP spectrogram.

(E) Characterization of UP states within nonREM. See Supplemental Experimental Procedures for details of identification algorithm. Top: average wavelet spectrum of LFP from UP states normalized in time for comparison (0 to 1). Middle: mean firing rates of the putative pyramidal cells and interneurons during normalized and averaged UP states from all sessions and all rats. Bottom: population synchrony of pyramidal cells (fraction of spiking neurons in 50 ms bins) and the ratio of the fraction of pyramidal cells and combined fraction of pyramidal cells and interneurons in 50 ms bins (E/E+I ratio) during normalized UP states from all sessions and all rats.

orders of magnitude range from 0.05 Hz to 5 Hz (Figure 2A). Median rates (± SD) of putative pyramidal cells in each state were as follows: WAKE, 0.76 ± 1.53 Hz; nonREM, 0.69 ± 0.86 Hz; REM, 0.88 ± 1.33 Hz; and for putative interneurons were as follows: WAKE, 5.59 ± 7.25 Hz; nonREM, 4.69 ± 5.62 Hz; REM,

4.25 ± 9.43 Hz. Whereas nonREM and WAKE firing rates remained highly correlated on a per-cell basis (R = 0.82, p < 1^{-10}), the slope of this relationship significantly deviated from 1 (Figure 2B), demonstrating that state transitions exert a differential effect across the firing rate spectrum (slope, 95% confidence
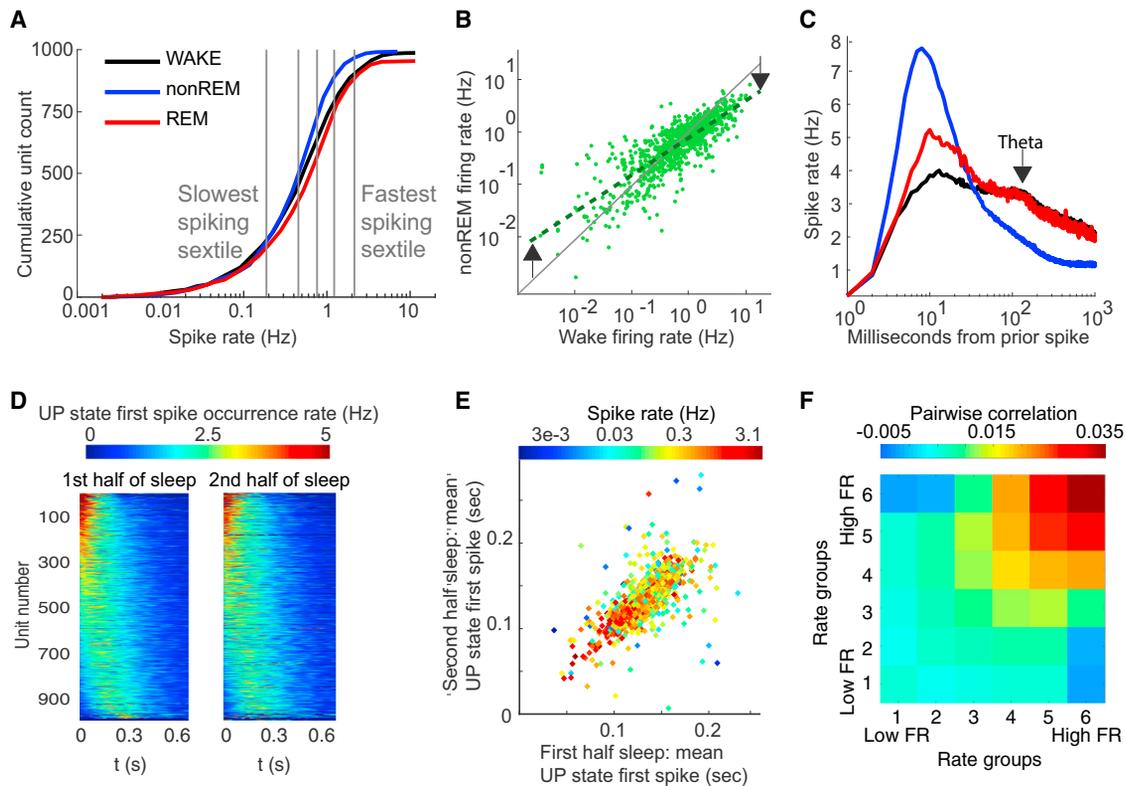
Figure 2. Cortical Neuronal Firing Patterns in Different States

(A) State-wise differences of average firing rate. Cumulative distribution of the firing rates of individual putative pyramidal neurons (log scale). Note brain-state-dependent differences (color). Vertical lines separate equal number of neurons into six subgroups (sextiles) based on WAKE firing rate—used in later analyses.

(B) Differential effect of brain state on neurons of different firing rates. Comparison of the firing rates (log scale) of the same pyramidal neurons during WAKE and nonREM—each point is the same neuron in two states. During nonREM, neurons at the right end of the distribution are decreased, but neurons at the left end of the distribution increase their rates compared to WAKE (arrows).

(C) Temporal relationships of spikes across brain states. Average single-cell spike autocorrelogram shows largest peak at 8 ms during nonREM and small peaks at 125 ms (~8 Hz theta frequency) during REM and WAKE (arrow) and a fast decay of spiking, especially in nonREM.

(D) Spike timing in UP states is consistent. Cell-wise histograms of time-resolved likelihood distribution of the first spike time fired by each pyramidal neuron across all DOWN-UP state transition (set to 0 ms) shown separately for the first and second halves of SLEEP episodes. Color represents the normalized firing likelihood for that unit. Each unit is a horizontal color line, vertically sorted identically in both columns by the mean onset time during the first half of SLEEP.

(E) UP state spike timing correlates with cell firing rate. Comparison of the mean latency to the first spike of each neuron during the first and second halves of the recording session (same data as D). Note that faster-firing neurons tend to fire at shorter latencies.

(F) Firing rate predicts cofiring. Mean pairwise correlation of pairs of neurons in nonREM sleep based on 100 ms bins, separated into six firing rate groups based on mean rate. Note high correlations between high firing rate pairs of cells and negative correlation between slow- and fast-firing neuron pairs. All comparisons, except 4,4, are significant (see Supplemental Experimental Procedures).

interval 0.66–0.71). The right tail extended toward higher rates during WAKE and REM compared to nonREM (Figure 2A; fraction of >2 Hz neurons, WAKE = 19.2%, REM = 19.2%, nonREM = 8.8%; chi-square test, all comparisons $p < 1^{-10}$).

In addition to single spikes, pyramidal neurons also fire spike bursts (Connors and Gutnick, 1990; Steriade et al., 2001). Here we defined the burst index as the fraction of spikes with interspike intervals <15 ms. Burst index was highest during nonREM (median in nonREM = 11.8%) and lowest during WAKE (4.0%), with REM (5.5%) slightly higher than WAKE ($p < 0.05$; Kruskal-Wallis test). State dependence of firing patterns was also evident in the averaged autocorrelograms of single units: a large peak occurred at approximately 8 ms interspike interval during nonREM, whereas smaller peaks were present at ~125 ms (i.e., theta frequency) during REM and WAKE (Figure 2C). These

data are consistent with intracellular recordings (Steriade et al., 2001). Time decay of the autocorrelograms of pyramidal neurons was significantly faster during nonREM compared to WAKE and REM (Figure 2C; decay fit exponent median, nonREM = −1.35, WAKE = −0.83, REM = −0.80; $p < 0.05$; Kruskal-Wallis test). Putative interneurons tended to sustain similar activity across brain states (Figures S2C–S2E). Because of their smaller number and high variability, interneurons were not analyzed in detail.

Population-level firing patterns also varied across brain states. The fraction of principal cells firing in 50 ms overlapping time windows (population synchrony) showed a skewed distribution. More than 15% of principal neurons rarely fired synchronously with others (4% of windows), while less than 4.2% discharged synchronously in at least half of the windows. Furthermore, analyzing synchrony among populations in different states

(Figure S2F) revealed brain-state-dependent differences in the distribution of synchrony over time windows. NonREM was characterized by a large fraction of time windows with all neurons silent, corresponding to DOWN states alternating with nonsilent UP states. The durations of DOWN states of slow oscillations showed a skewed distribution (median = 0.19 s) and so did the UP states (median = 0.47 s; Figure S4A). UP states were characterized by an initial surge of gamma power, followed by increased sigma power (Figure 1E), corresponding to UP-state-related sleep spindles. Firing rates of both pyramidal cells and interneurons decreased over the time course of the UP state, accompanied by a decreasing gain of excitation (excitatory-inhibitory [E-I] ratio) and decreasing population synchrony of pyramidal neurons (Figure 1E).

In agreement with previous reports (Luczak et al., 2007), pyramidal neurons fired in reliable spatiotemporal sequences during the early part of the UP state (<200 ms), and these stereotypical sequences remained stable across the entirety of sleep (Figure 2D). Additionally, the spike onset times of individual neurons in the sequences were negatively correlated with their firing rates (Figure 2E) (Peyrache et al., 2010). To explore this relationship further, we arbitrarily sorted neurons into six firing rate groups and assessed average pairwise correlations of spiking between all combinations of these groups within nonREM sleep (Figure 2F). Seemingly as a result of the "fast before slow" relationship seen in spike timing during UP states (Figure 2E), the fastest- and slowest-firing neurons tended to be positively correlated within groups but were actually negatively correlated across groups (Figure 2F).

Firing Pattern and LFP Changes across the Course of Sleep

We identified 54 WAKE-SLEEP episodes in our dataset, or an average of 2.0 episodes per neuron recorded (27 sessions), and analyzed changes on a per-episode basis. In agreement with previous studies (Grosmark et al., 2012; Vyazovskiy et al., 2009), we found that the arithmetic mean of the population firing rates of pyramidal cells declined over the course of sleep using a test of correlation of spike rate versus time (Figures 3A and 3B; $R = -0.11$, $p < 10^{-3}$). Comparison of the population discharge rates in the first and last nonREM packets of SLEEP episodes showed an overall mean rate decrease (1.04 ± 1.20 Hz versus 0.88 ± 0.91 Hz; $p < 0.02$; Wilcoxon test) (Vyazovskiy et al., 2009). This effect was "carried over" to subsequent WAKE, as shown by the significantly decreased discharge rate of pyramidal neurons in a 5 min postsleep WAKE compared to a 5 min presleep WAKE epoch ($p < 10^{-6}$; Wilcoxon test).

By contrast, within-neuron comparisons demonstrated that sleep brings about systematically varying effects across the rate spectrum: while fast-firing pyramidal neurons decreased rate over SLEEP, slow-firing neurons increased their rates (Figure 3D). To quantify this observation, we assessed spike rates of the same neurons in the first versus the last nonREM packets of SLEEP and found the slope of this correlation significantly departed from unity (slope, 95% confidence interval 0.827–0.880). This "tilting" of the slope of fit demonstrates that high firing rate neurons tend to decrease their firing rates while the low firing rate neurons tend to elevate their firing rates over sleep. This echoed the differential firing shifts observed in the state transition from WAKE to nonREM (Figure 2B). To further characterize this differential effect, we divided pyramidal cells from across the dataset into six sextile groups based on their WAKE firing rates (Figure 2A). We maintained these firing rate groups for all subsequent analyses. Since the duration of SLEEP varied across rats and sessions, sleep session lengths were time normalized for group comparisons (Grosmark et al., 2012). Additionally, we only included nonREM periods in our analysis to control for state-related rate shifts. The mean spike discharge rate of highest firing rate sextile groups significantly decreased over sleep, whereas the activity of the lowest firing rate sextile showed a marginal increase (Figure 3B; Pearson correlations versus normalized time). In agreement with the differential rate changes of the sextile groups, the coefficient of firing rate variation also showed a significantly decreasing slope over the course of SLEEP ($R = -0.05$; $p < 0.01$).

Parallel with the spike rate shifts, multiple other parameters showed gradual changes over the course of SLEEP (Figure 3C), analyzed on a per-SLEEP epoch basis, and again confined to nonREM periods. Incidence of spindles (1.94 ± 0.39/min) decreased ($R = -0.093$; $p < 10^{-5}$), while spindle duration (0.52 ± 0.32 s), frequency (13.93 ± 0.93 Hz), and amplitude (203.3 ± 87.71 μV) did not change over SLEEP. Incidence of both UP states ($R = -0.10$; $p < 10^{-6}$) and DOWN states ($R = -0.08$; $p < 10^{-4}$) decreased significantly, while the duration of DOWN states increased ($R_{slope} = 0.09$; $p < 10^{-4}$; Figure 3B) and duration of UP states did not change. In addition, the fraction of time that could be identified as neither UP nor DOWN state (other) increased significantly over the course of sleep ($R = 0.08$; $p < 10^{-2}$), implying changes in overall UP-DOWN drive. Comparison of firing rates within UP states showed a general decrease across the whole population (Figure S3C), and subtraction of UP state firing activity in early sleep from that in late sleep revealed that the firing rates of the fastest sextile group and putative interneurons decreased later in sleep, whereas firing of the slowest sextile increased (Figure 3F). These results reveal that UP/DOWN changes themselves are not the sole factor in determining spike rate changes across sleep, but there are within-UP-state effects that play a strong role.

Finally, we analyzed how firing rates changed from the first to the last epoch of MA and REM, to complement our nonREM analyses. We again found that changes from the first to last REM episode or the first to last MA demonstrated differential effects across the rate spectrum, with higher firing rate neurons decreasing firing rate and low firing rate neurons increasing toward the end of sleep (Figure S3A).

Together, these findings demonstrate that instead of downscaling and eliminating slow-firing neurons (i.e., reducing their rates to zero) (Tononi and Cirelli, 2014), sleep brings about a spike rate homogenization effect by upscaling the slow-firing neurons and decreasing the activity of fast-firing neurons. In the next set of analyses, we investigated potential mechanisms responsible for these differential rate changes.

Firing Rate and LFP Changes within NonREM Episodes and Packets

To better understand the changes occurring across sleep, we took the approach of analyzing changes within specific sleep
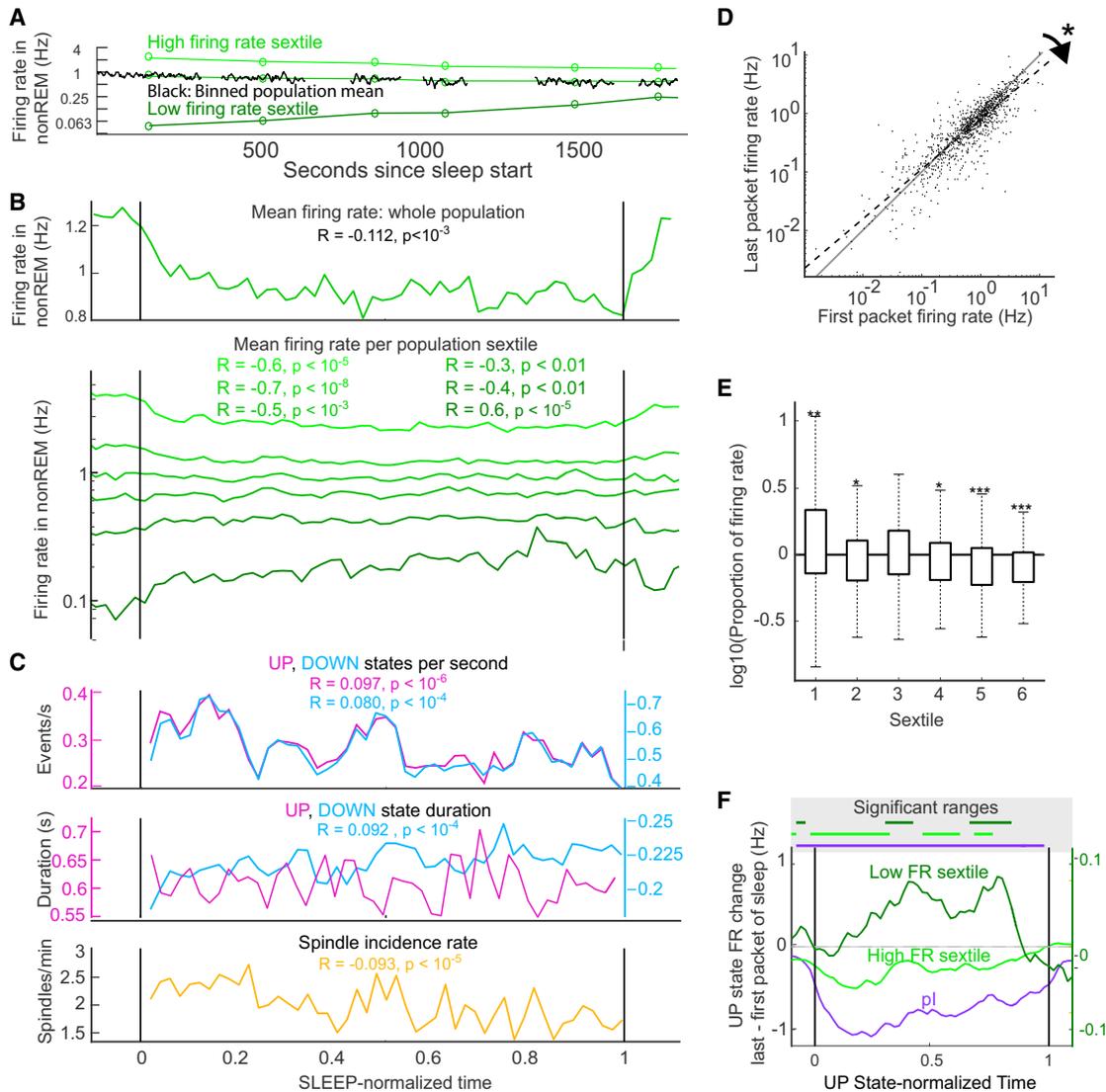
Figure 3. Firing Pattern Changes over the Course of SLEEP

(A) Example of opposite modulation of firing rate over sleep. Population mean firing rates (black traces), and mean packet firing rate for the fastest- and slowest-firing sextiles (green circles) of pyramidal neurons in an example session. Only nonREM packets are shown for clarity. High firing rate cells show downregulation over sleep; low firing rate cells increase firing over sleep.

(B) Firing rate changes across sleep. Top panel: population arithmetic mean firing rate. R, slope of the rate change within time-normalized sleep from all neurons in all recordings (n = 995 cells; n = 54 sessions; 11 rats). Bottom panel: firing rate changes in each of six groups defined by WAKE firing rate (see Figure 2A), all cells and all sessions. R and p values for correlations of each mean firing rate versus normalized time are shown in colors corresponding to plot for each sextile. Measures are per restricted to nonREM; therefore, changes are not due to relative ratios of nonREM to REM/MA. High firing rate neurons show decreasing activity; low firing rate cells increase activity over sleep.

(C) Slow oscillations and spindles over SLEEP. UP and DOWN state occurrence rates (top) and UP and DOWN state durations (middle) within SLEEP. Bottom: spindle incidence. UP state duration not significantly correlated with time; all other significances shown, including decreasing UP, DOWN, and spindle occurrence rates. All values are restricted to nonREM times to control for state changes over sleep.

(D) Opposite modulation of neurons of different firing rates. Comparison of individual neuron firing rates during the first and last packets of SLEEP. The regression line is significantly different from unity (slope, 95% confidence interval 0.83–0.88), showing that high and low firing rate neurons are oppositely modulated over sleep.

(E) Firing rate changes from SLEEP persist into subsequent WAKE. Comparison of sextile-wise firing rates during the 5 min of WAKE before versus the 5 min of WAKE after SLEEP. Asterisks above bars indicate significance of one-tailed Wilcoxon, *p < 0.005, **p < 0.001,***p < 0.0001. Boxes indicate 25–75 percentile range; error bars show most extreme values in each distribution.

(F) Within-UP state firing rate changes across SLEEP. Lines correspond to the difference of UP state values of last versus first packets of SLEEP. Putative inhibitory (pI) and excitatory cells (pE) from the fastest sextile showed a rate decrease, whereas the slowest sextile (right y axis) showed an increase over SLEEP. We also show time-resolved changes across the span of the average UP state (0 to 1 on abcissa).

substate epochs. We begin with nonREM sleep, which has been the point of focus in the sleep homeostasis literature. We classified nonREM into the more classical nonREM episodes that occur between WAKE and REM epochs (but which may have some interruptions by MAs of up to 40 s duration) and nonREM packets that are the noninterrupted periods of pure nonREM found within nonREM episodes. Despite their approximately 3-fold difference in timescale, we found that nonREM episodes and packets were characterized by very similar dynamics as each moved from start to completion (Figure 4). Our first analyses involved LFP features of these states. Power-power correlations of LFP features during nonREM sleep (Figure S1B) identified three independently varying frequency bands: delta (0.5–4 Hz), beta or sigma (9–25 Hz), and gamma (40–100 Hz); subsequent LFP analyses were based on these three independent bands.

Over nonREM episodes and packets, delta and sigma band power steadily increased (Trachsel et al., 1988), whereas gamma power decreased over episodes, but not packets (Figures 4A and 4Bi). This latter finding was the only qualitative difference noted between episodes and packets. Mean delta power within whole packets (normalized by nonREM delta power) was positively correlated with packet length ($R = 0.31$; $p < 0.05$). Since spectral analysis only indirectly describes the dynamics of slow oscillations (Campbell and Feinberg, 1993; Steriade et al., 1993), we also calculated LFP features of slow oscillations (Figures 4A and 4Bii). The incidence of both UP states ($R = 0.05$; $p < 10^{-3}$) and DOWN states ($R = 0.08$; $p < 10^{-10}$) increased significantly within packets, whereas the duration of UP states decreased ($R = -0.02$; $p < 0.01$) and DOWN states increased ($R = 0.07$; $p < 10^{-10}$), changing the UP-DOWN balance (UP/DOWN ratio negative correlation versus time $p < 0.05$). The fraction of epochs identified as neither UP nor DOWN (see Supplemental Information) increased over packets ($R = -0.04$; $p < 10^{-3}$).

The incidence of spindles significantly increased both within nonREM episodes (Figures 4A and 4Biii; $R = 0.08$; $p < 10^{-10}$) and packets ($R = 0.7$; $p < 10^{-10}$). Spindle duration also increased (nonREM episode increase from 0.61 ± 0.33 s to 0.67 ± 0.30 s; $R = 0.08$; $p < 10^{-3}$; nonREM packet increase from 0.58 ± 0.25 s to 0.67 ± 0.27 s; $R = 0.07$; $p < 10^{-4}$), whereas spindle frequency and amplitude remained unchanged. Thus, the changes within nonREM did not necessarily reflect changes in the same metrics across SLEEP, implying different mechanisms.

During the final portion of packets, the generally positive correlation between delta and sigma power was replaced by a sudden increase of sigma power and concurrent decrease of delta power (Figures 4A and 4Bi). Furthermore, sigma power was elevated in late-packet UP states, as shown by the significant difference of sigma power between DOWN-UP transition-triggered spectrogram in the late versus early parts of nonREM packets (Figures 4E and S4B; $p < 10^{-5}$; t test).

Firing rates of pyramidal cells also changed within nonREM episodes and packets. Firing rates of the fastest-firing sextile groups decreased, whereas those of the slowest-firing sextile groups increased within both nonREM episodes and packets (Figures 4A and 4Biv; R and p values in figure), resulting in a decreasing coefficient of variation of binned population firing

rates (Figures 4A and 4Bv; $R_{episode} = -0.13$, $p < 10^{-10}$; $R_{packet} = -0.12$, $p < 10^{-10}$). An additional metric, the 15 ms spike burst index of pyramidal neurons, also showed a positive slope within both nonREM episodes and packets (Figures 4A and 4Bvi; $R_{episode} = 0.09$, $p < 10^{-10}$; $R_{packet} = 0.08$, $p < 10^{-10}$).

Next, we addressed the relationship between firing rate and LFP metrics within nonREM packets by assessing how packet-wise firing rates (normalized per sleep session) correlated with LFP metrics of those packets. Per-packet firing rate of the top sextile group was negatively correlated with per-packet LFP metrics, including whole-packet delta power (Z scored per session; Figure 4C; $R = -0.28$; $p < 10^{-10}$), DOWN state duration ($R = -0.16$; $p < 10^{-4}$), and DOWN state incidence rate (Z scored per session; $R = -0.29$; $p < 10^{-10}$). A positive correlation was observed between firing rate of the top sextile group and UP state duration ($R = 0.14$; $p < 10^{-3}$) and gamma power (Figure 4D; $R = 0.44$; $p < 10^{-10}$). Finally, a positive correlation was found between normalized firing rates per packet in the bottom sextile group and sigma power in the last 20 s of the packet ($R = 0.25$; $p < 10^{-10}$). Other tested relationship combinations were not significant. In summary, only fast-firing neurons were negatively correlated with DOWN state features and positively correlated with UP state features on a per-nonREM packet basis. On the other hand, lowest firing rate neurons were correlated with packet-end sigma power.

Since nonREM is dominated by UP/DOWN state shifts, we examined LFP and firing rate changes within UP states themselves. Spectral comparison of UP states in first third versus last third of packets showed increased sigma power in later UP states (Figure 4E; $p < 10^{-10}$; Wilcoxon rank-sum test and per-pixel significance; Figure S4B). Comparison of within-UP-state activity in the first versus last third of packets showed a drop in firing rate for the fastest sextile group ($p < 10^{-8}$; Wilcoxon rank-sum test), an increase in firing rate of putative interneurons ($p < 10^{-3}$), and a small but significant decrease for the slowest-firing group ($p < 0.003$; Figures 4B and 4E). Thus, firing rate changes within nonREM packets were not simply due to changes of UP state and DOWN state durations or ratios within packets.

Finally, we analyzed intrastate changes of firing rates within REM and WAKE states using the same sextiles employed above. We found that entry into WAKE corresponded with an increase in firing rate of the highest two sextile groups and a drop in firing rate of the lowest two sextile groups (Figure S5A), opposing the effects seen in SLEEP and nonREM. During REM, all sextile groups except the fourth showed an increase in firing rate (Figure S5B), consistent with the distinction between REM and WAKE, despite superficial similarities.

We find that within-nonREM neurons are regulated in a manner similarly to within SLEEP. WAKE appears opposite to SLEEP and nonREM in terms of differential effects on neurons of different spike rates.

Sleep Substates Induce Differential Lasting Firing Rate Changes

The above analyses did not reveal which, if any, of these changes persist beyond each state into subsequent brain states. To test this, we utilized triplets of the type state A_n- state B- state

A nonREM episodes

B nonREM packets

i) Zscore

ii)

iii)

iv)

v)

vi)

C High FR sextile

D

E Zscore
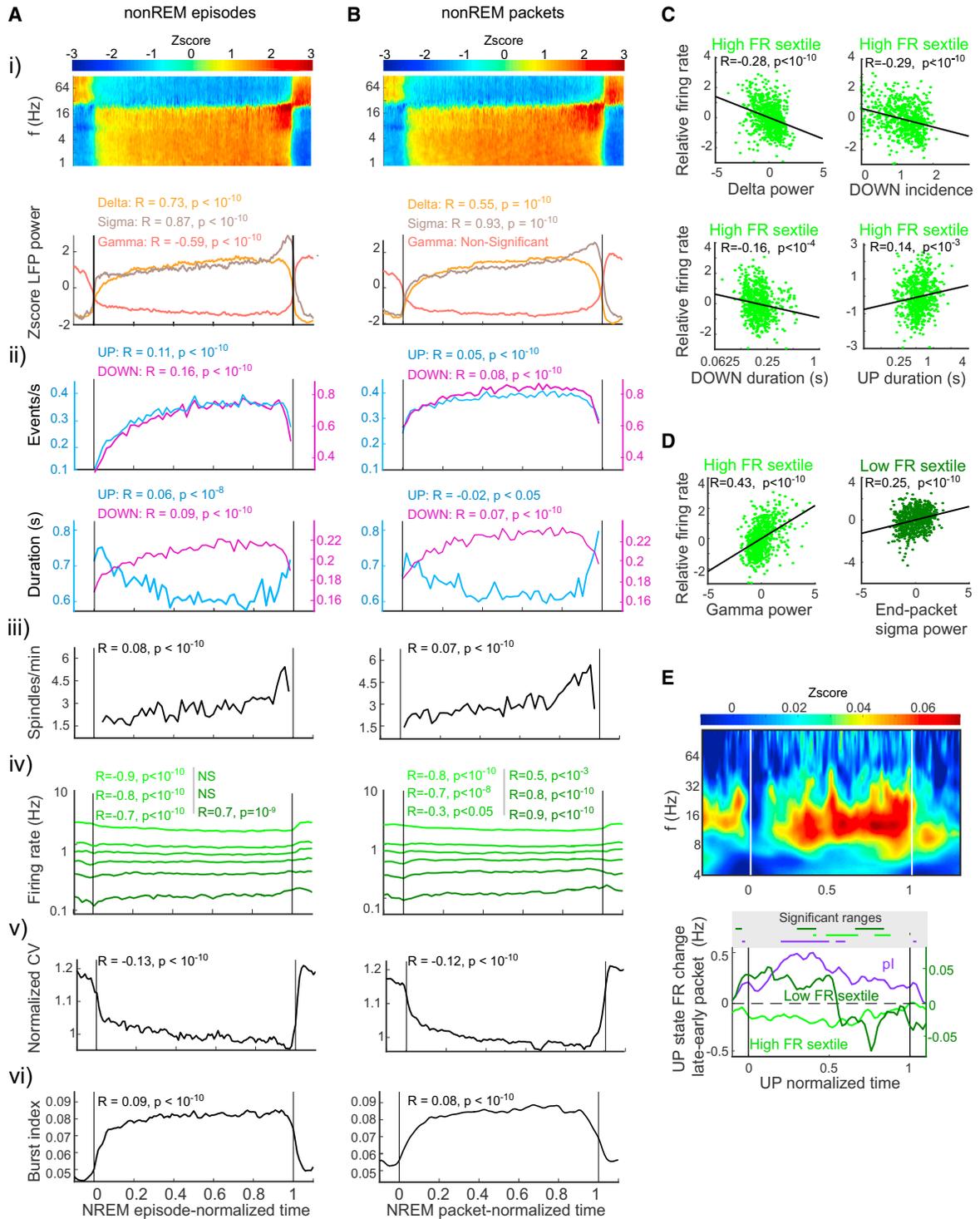
Figure 4. Comparison of Changes within NonREM Episodes and NonREM Packets

(A and B) Comparisons of metrics across (A) time-normalized nonREM episodes and (B) time-normalized nonREM packets. All R and p values of metrics versus normalized time are displayed above data.

(i) Time-normalized spectrogram (top) and evolution of delta (1–4 Hz), sigma (9–25 Hz), and gamma (40–100 Hz) power (bottom) within nonREM episodes and packets.

(ii) Evolution of UP and DOWN state incidence and duration.

(iii) Spindle incidence.

(legend continued on next page)

A_{n+1}. We quantified changes from the n to the n + 1 occurrence of state A, and we attributed changes to the intervening state B.

We started by testing whether the sextile-wise changes within SLEEP were carried over to WAKE after the termination of SLEEP. Comparison of firing rates during 5 min of WAKE immediately before SLEEP versus 5 min of WAKE immediately after SLEEP showed a significant decrease in firing in the top three sextile groups and an increase in the lowest sextile group (all $p < 0.05$; stars in Figure 3E). We also found an inverse correlation between baseline firing rate and change in spike rate from WAKE before to WAKE after sleep (Figure S3A; slope, 95% confidence interval 0.801–0.0856).

To examine the lasting impact of nonREM packets, the difference between sextile group firing rates in MA_{n+1} and MA_n was compared on either side of individual packets. Firing rates in the top two firing rate sextiles were significantly reduced by the intervening nonREM packet (both $p < 0.01$; Figure 5B, blue), confirming previous reports that nonREM and WAKE have opposite effects on firing rates (Grosmark et al., 2012; Vyazovskiy et al., 2009). Analysis of rate change versus firing rate for these triplets also showed an inverse correlation between rate and change (Figure S5C), as did a similar analysis for REM_n- packet- REM_{n+1} triplets (Figure S5D). Additionally, we found that sigma power in the last 20 s of nonREM packets was correlated with a greater increase in the lowest firing rate sextile group in the MA_n versus MA_{n+1} analysis (Figure 5C; $R = 0.181$; $p < 0.01$).

Next, we assessed differential effects of WAKE versus MA versus REM by measuring firing rates in successive nonREM packets ($packet_n$ versus $packet_{n+1}$) straddling each of these states (Figure 5B). WAKE episodes increased the activity of the fastest-firing sextile group of pyramidal cells from nonREM $packet_n$ to $packet_{n+1}$ (Figure 5B, black). Furthermore, WAKE periods with more movement had a proportionally larger effect (Figure 5C; $R = 0.43$; $p < 0.05$). WAKE also appeared to exert a rate-decreasing effect on slow-firing neurons, although this effect was not significant; similarly, a correlation of rate versus log percent change was also not significant (Figure S5E), possibly due to the small number of uninterrupted nonREM-WAKE-nonREM triplets (n = 24).

In contrast to WAKE, MA epochs between packets did not affect fast-firing neurons but significantly increased the rate of slow-firing neurons from $packet_n$ to $packet_{n+1}$ (Figure 5B, yellow). Again, the differential effect across sextiles was confirmed by a correlation analysis (Figure S5G). Finally, REM episodes decreased the spike rates from $packet_n$ to $packet_{n+1}$ in all sextile groups (Figure 5B, red). Longer REM episodes exerted a propor-

tionally larger effect on rate changes from $packet_n$ to $packet_{n+1}$ for all sextile groups (Figure 5C; $R = -0.22$; $p < 10^{-2}$; t test), and REM theta power was significantly correlated with the $packet_n$ to $packet_{n+1}$ rate decrease of the slowest sextile group only ($R = -0.15$; $p < 0.05$). Correlational analysis did not reveal differential effects of REM on neurons across the rate spectrum (Figure S5F). We also found a more general interaction between firing rate and delta power changes from $packet_n$ to $packet_{n+1}$ when analyzing, regardless of intervening state. The increase of spike rate from $packet_n$ to $packet_{n+1}$ in the slowest sextile group was positively correlated with the delta power change from $packet_n$ to $packet_{n+1}$ (Figure 5C).

Many of the within-state effects seen in our earlier analyses carried over to subsequent states. Overall, despite all being considered arousal-like states, WAKE, MA, and REM exerted qualitatively and quantitatively different effects on neuronal spiking. Furthermore, many of the effects observed across states were correlated with measurable aspects of those states, substantiating the role of the state itself as a mechanism of spike rate change. Specifically, WAKE states increased the activity of the highest rate group, whereas nonREM sleep opposed this effect. MA, by contrast, preferentially increased the discharge rate of slow-firing neurons, whereas REM sleep decreased the rate of all principal cells by approximately the same proportion (Figures 5 and 6).

DISCUSSION

By sampling large numbers of neurons, we show that pyramidal cells in frontal cortex have a strongly skewed, wide dynamic range of firing rates and that the various substates of sleep differentially affect neurons at different ends of that firing rate distribution (Figure 6). Furthermore our simultaneous sampling revealed that a primary goal of sleep-based regulation is modifying the instantaneous width of this distribution. During nonREM, activity of fast-firing neurons decreased, whereas activity of slow-firing neurons increased. REM sleep reduced firing rates relatively uniformly across firing rate groups, whereas MAs, interspersed between nonREM epochs, increased the discharge rates of slow-firing neurons. Accordingly, the net result of sleep is that the firing rate variation of the population is decreased. These experimental findings cannot be accounted for by the current homeostatic models and provide novel insight into how different aspects of sleep cooperate in adjusting network excitability toward a central value. Our results support the idea that neurons at different ends of the firing rate spectrum may have different roles in network function.

(iv) Firing rate changes in the sextile groups.
(v) Coefficient of variation of within-session population firing rates.
(vi) Incidence of spike bursts (fraction of spikes with <15 ms intervals).
(C) Correlation between packet delta oscillation parameters and within-nonREM packet firing rate. High firing rate neurons show significant negative correlations with slow-wave metrics, with the exception of a positive correlation with UP state duration. Low firing rate neurons do not show significant correlations.
(D) Sigma and gamma band correlates of firing rate. Gamma power in packets correlates with higher firing rate in high-rate cells. Low firing rate neurons fire more in packets with higher sigma-band power at the end of the packet.
(E) Within-UP state changes across nonREM packets. Top: subtraction of spectrogram of last third of packets from that of first third of packets. Note increased spindle power at the end of nonREM packet, which is present throughout UP state duration. Bottom: spike rate changes from first to last thirds of packets of the top and bottom sextiles of putative excitatory (pE) units and putative inhibitory (pI) units. Note that pI units increased their within-UP state firing later in packets, whereas the fastest sextile of pyramidal cells decreased their rates.
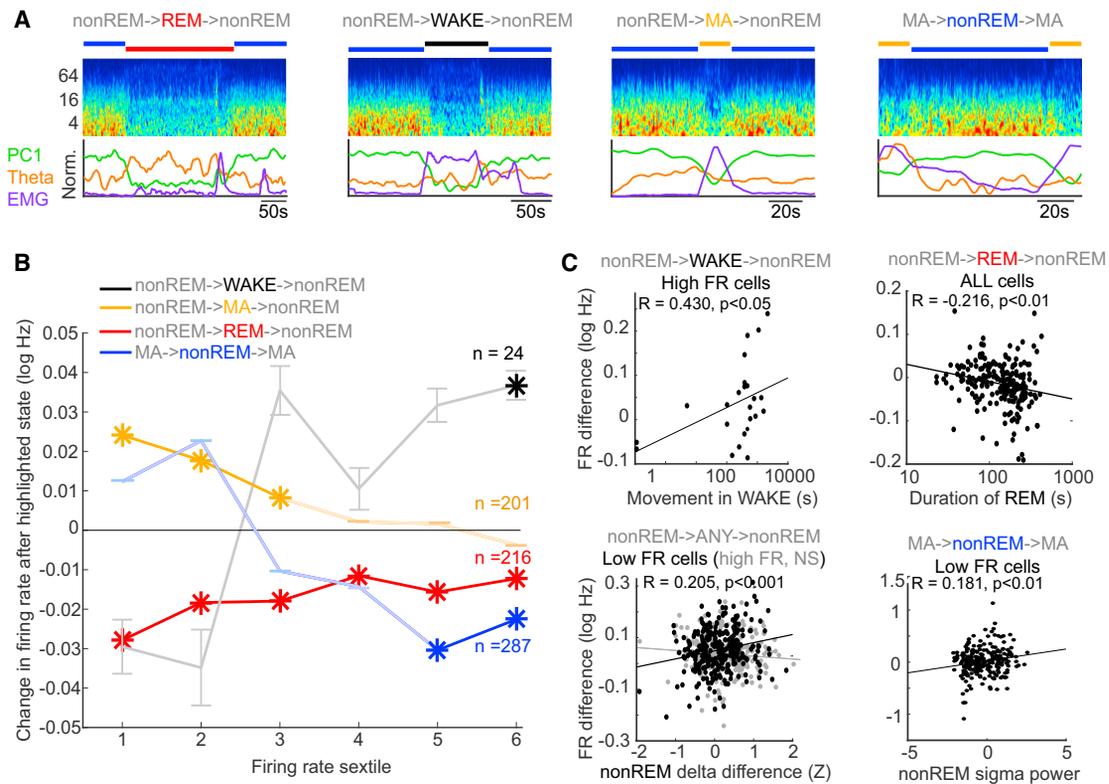
Figure 5. Persisting Effects of WAKE, REM Sleep, and MA on Firing Rates

(A) Examples of state triplets involving two iterations of a state spanning an intervening state. Scored states are indicated above time-resolved FFT spectrum of the LFP for each example. Below spectrograms are shown the PC1 power, EMG power, and theta power metrics used in state scoring.

(B) Persisting rate changes across state triplets. Black, red, and yellow plots show firing rate changes in the sextile groups between $nonREM_n$ and $nonREM_{n+1}$ epochs respectively spanning WAKE, REM, or MA states. Changes from subtraction of average per-cell firing rate in $nonREM_n$ from $nonREM_{n+1}$ are plotted for each firing rate sextile and are attributed to effects of the intervening state. Asterisks indicate significant change. Also shown are the firing rate changes between MA_{n+1} and MA_n brought about by intervening nonREM state. Noted are n's for each class of triplet; error bars represent SEM for all points. While WAKE brings up spiking of high firing rate cells, nonREM brings down the firing rate of that group. MAs elevate spiking of low firing rate cells, and REM reduces spike rates across the firing rate spectrum.

(C) Correlates of rate change magnitudes across state triplets. Upper left: degree of movement within WAKE correlates with degree of rate increase in the highest firing rate sextile group. Upper right: duration of REM correlates with degree of firing rate drop across all cells. Lower left: difference in delta power between consecutive packets (calculated as within-session normalized delta power), regardless of intervening state, correlates positively with degree of spike rate change in the lowest firing rate sextile. Same finding not replicated in highest firing rate sextile. Lower right: sigma band power in the last 20 s of a packet between two MAs correlates with the increase in firing of the lowest firing rate sextile group from one MA to the next.

Modulation over SLEEP

Although we confirmed that the overall firing rate is decreased during sleep (Vyazovskiy et al., 2009), we show that this effect is due to the decreased activity of the fastest-spiking minority of neurons. By contrast, we also found that SLEEP increased the activity of slow-firing neurons, with an overall result of homogenization of population rates. Other reports show changes in the coefficient of variation of the amplitude of miniature excitatory postsynaptic currents in vitro, indicating homeostasis can work similarly on synaptic weights (Thiagarajan et al., 2005).

Homeostatic regulation based on a uniform directionality of modulation of all network elements has been seen in some experimental paradigms and could have various mechanisms. First, global synaptic scaling (Turrigiano et al., 1998) may be brought about by activity-dependent diffusion of substances (Rutherford et al., 1998; Stellwagen and Malenka, 2006). Alterna-

tively, cortical neurons could sense their own firing patterns and globally adjust synaptic strength (Buzsáki et al., 2002) via intracellular signaling and transcription (Ibata et al., 2008). However, uniform synaptic scaling may produce instability in recurrent circuits (Blanco et al., 2015; Buonomano, 2005; Kim and Tsien, 2008; Mitra et al., 2012). Although previous modeling has predicted a diversity of plasticity effects (Blanco et al., 2015), our experiments represent a rigorous description of the regulation of neuronal activity spanning the firing rate spectrum in natural sleep. Our findings demonstrate that neurons with different firing rates are differentially but cooperatively regulated by the substates of sleep (Figure 6).

NonREM Sleep

During nonREM sleep, we see a spike rate homogenization similar to the overall sleep effect (Figure 2F). One factor

A

Sextile group number
(log firing rate)

1 2 3 4 5 6

WAKE

nonREM

REM

Micro-
arousal

SLEEP

B

WAKE

nonREM

REM

Micro-
arousal

SLEEP
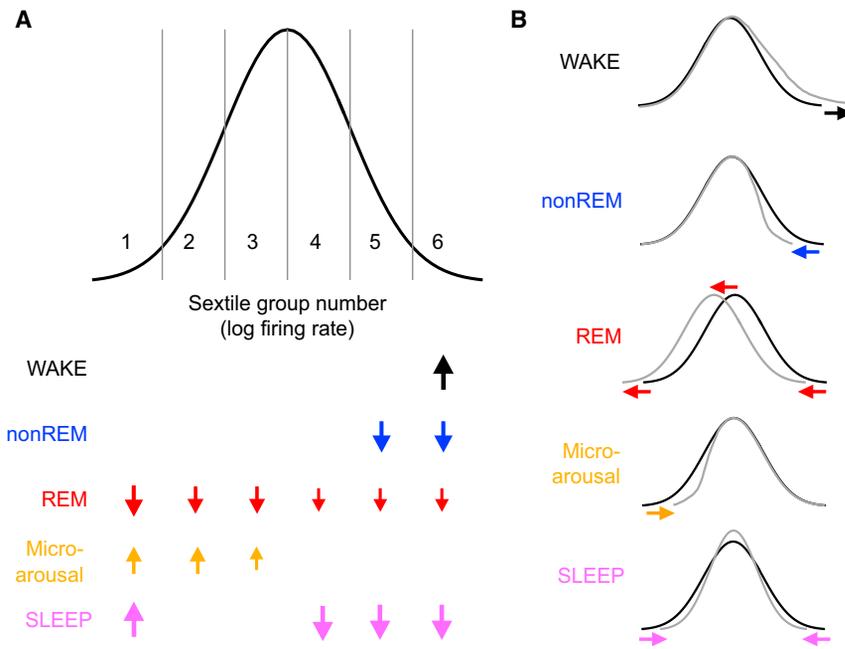
Figure 6. Effects of Brain States on Neural Firing Rates

(A) Idealized distribution of the log firing rates of cortical neurons, divided into six sextiles to match our analyses here. Lower: chart of significant persisting changes by state and by firing rate sextile. Arrow size indicates the magnitude of the observed significant effects on firing rate of WAKE, nonREM, REM, and microarousal (MA) states on subsequent states, based on numbers from Figure 5B. In addition, the rate changes brought about by SLEEP relative to WAKE are also shown (bottom), based on numbers from Figure 3E. Note that the overall effect of SLEEP is mimicked by the combination of the contributions of multiple substates of sleep.

(B) Each panel illustrates the impact of one brain state (color coded) on the idealized distribution of population firing rates.

contributing to the inverse relationship between high and low firing rate cells may be the fact that spiking in nonREM is largely restricted to UP states, and fast-firing neurons tend to fire earlier and slow-firing neurons tend to fire later in those events (Luczak et al., 2007; Peyrache et al., 2010). This "fast before slow" pattern during UP states is a potential mechanism for differentially affecting synapses between neurons occupying the left and right parts of the firing rate distribution. Since fast-firing neurons tend to fire first, they are less likely to undergo potentiation by spike-timing-dependent plasticity (STDP) (Markram et al., 1997) than the later-firing slow-firing cells. Furthermore, since the synaptic strength change by the STDP rule depends strongly on the firing rate of the postsynaptic neuron, fast-firing neurons are less able to potentiate than slow-firing cells (Bienenstock et al., 1982; Lim et al., 2015). By these combined mechanisms, the UP state can function as a rate "segregator" since it temporally separates neurons by their spike rates (Luczak et al., 2015).

Neuromodulators may also support the rate-reducing effect of nonREM on the high-firing neurons. Whereas strong synaptic excitation during UP states can increase membrane conductance and lead to selective reduction of synaptic potentiation without affecting synaptic depression, in vitro β-adrenergic receptor activation has been shown to reverse this effect (Delgado et al., 2010). This suggests that the shifting levels of norepinephrine and other subcortical neuromodulators that occur across sleep substates can shift STDP rules from depression to potentiation.

It should be emphasized that the rate decrease of fast-firing neurons within nonREM packets is not a simple consequence of the increased incidence and duration of DOWN states. First, UP state incidence also increased. Second, slow firing rate neurons showed an opposite change in firing rate. Third, when firing rates were considered only in UP states, rate decrease of fast-firing neurons from early to late nonREM packets was still pre-

sent. In contrast, firing rates of putative interneurons during UP states increased from the early to the late nonREM packets of sleep (Figure 4E). This latter finding is a strong argument against the possibility that the pattern changes of faster-firing putative excitatory neurons were due to any contamination by interneurons, which may be regulated by different mechanisms (Cohen et al., 2016).

REM Sleep

Despite within-REM firing rate increases, REM had a net persisting effect of down shifting firing rates of all neuron groups, a reflection of a mechanism involving proportional changes (i.e., division or multiplication) (Figure 6). Longer REM episodes exerted proportionally larger downscaling effects. Similar to previous observations in the hippocampus (Grosmark et al., 2012; Miyawaki and Diba, 2016), we found that WAKE and REM episodes exerted opposite effects on firing rates. Furthermore, whereas many minutes of waking activity are necessary for inducing lasting changes in firing rates during and after WAKE (Tononi and Cirelli, 2003, 2014), approximately a minute of REM had the same magnitude but opposite direction effect. This is of particular interest since WAKE and REM sleep are associated with seemingly similar network states. Whereas WAKE is strongly linked to elevated activity of cholinergic, serotoninergic, histaminergic, and noradrenergic neurons, during REM sleep only the cholinergic tone is high (Rasch and Born, 2013). It thus remains a possibility that serotonin and/or norepinephrine are responsible for producing different directions of rate changes during WAKE and REM (Delgado et al., 2010). Irrespective of mechanism, our findings provide further support for REM in downscaling excitability in cortical networks (Grosmark et al., 2012).

MAs and WAKE

MAs selectively increased firing rates of neurons at the low end of the firing rate distribution (Figure 6). Although MAs do not have a widely agreed-upon quantitative definition, they have been noted in numerous previous publications. In rodents, they

have been referred to as "low amplitude sleep" (Bergmann et al., 1987) and "low-amplitude irregular activity" (Pickenhain and Klingberg, 1967), whereas in humans the term MA was adopted (Halász et al., 1979). It could be argued that MAs are analogous or identical to the early part of WAKE before the animal displays overt behavioral features of waking, such as eye opening and movement, especially given the twitches of antigravity neck and masseter muscles and moderate increase of theta-band activity, compared to slow oscillations. Yet our findings demonstrate that MA is unique from WAKE. First, MA episodes were distinct from WAKE in terms of reduced theta/gamma power, closed eyes, and lack of whole-body movement. Second, whereas WAKE decreased the activity of slow-firing neurons, MAs increased it (Figure 6). A more quantitative characterization of the MA state requires further investigation, given its combination of clinical attributes (Douglas and Martin, 1996; Stepanski et al., 1984) and its unique role in cortical neuronal regulation as demonstrated here.

WAKE increased the firing distribution of pyramidal cells (Figure 6), with longer active WAKE episodes inducing stronger effects. Since our experiments were performed during the day, our experiments did not aim to examine global plasticity changes brought about by waking activity during the dark portion of the light cycle. Such comparisons are needed to disentangle the effects of sleep/waking from circadian effects (Dijk and Czeisler, 1995; Miyawaki and Diba, 2016).

Redistribution of Firing Rates during Sleep

According to the SHY model, neurons and synapses are overused after extended waking, and nonREM brings about recuperative changes by downscaling the network (Tononi and Cirelli, 2014; Vyazovskiy and Harris, 2013). Specifically, under this hypothesis neurons and synapses strongly activated during waking experience continue to be active during sleep, but weak synapses and slow-firing neurons are "down-selected" and functionally eliminated from network activity. This would allow for survival of "fittest" connections and neurons at the expense of weak ones (Tononi and Cirelli, 2014; Vyazovskiy and Harris, 2013). In contrast, the homeostatic scaling model (Turrigiano and Nelson, 2004; Turrigiano et al., 1998) assumes a uniform synaptic and rate adjustment by multiplying or dividing each synaptic strength and rate by the same factor. Since multiplicative scaling preserves the relative ratios between synapses and firing rates, it can keep the relative efficacy of learning-induced local modifications and preserve the selectivity of a neuron to different inputs (Miller, 1996; Rabinowitch and Segev, 2008; Turrigiano and Nelson, 2004).

In the SHY model, the DOWN state of slow oscillation plays a central role: "periods of reduced synaptic input ('off periods' or 'down states') are necessary" for downscaling synapses and firing rates (Vyazovskiy and Harris, 2013). The DOWN state is considered to be a corrective or prophylactic process that "shuts down" neurons to prevent metabolic damage from overwork. However, it is not clear how silencing of the network would downscale synaptic weights and firing rates. According to the homeostatic scaling model (Turrigiano and Nelson, 2004), prolonged silencing of neurons leads to a rebound elevation of spiking (Brailowsky et al., 1990). Prolonged network silencing after cortical deafferentation was suggested to be the cause of

trauma-induced epileptic excitability (Avramescu and Timofeev, 2008). In contrast to the hypothesized coupling between downscaling and slow oscillations (Tononi and Cirelli, 2003; Vyazovskiy and Harris, 2013), we found an inverse correlation between various features of slow oscillations and firing rates of fast-firing pyramidal neurons, coupled with a positive correlation with slow-firing neurons, resulting in a decreased dispersion of population firing rates (Figure 6).

The increased activity of slow-firing neurons during sleep is in disagreement with a core implication of the SHY model, which implies that sleep should eliminate slow-firing neurons by the repeated silencing of network activity during slow oscillations of nonREM (Tononi and Cirelli, 2014; Vyazovskiy and Harris, 2013). Furthermore, MAs of nonREM boosted the activity of slow-firing neurons, whereas WAKE and REM had the opposite effect on these cells. An acknowledged caveat is that while SHY is based largely on synaptic plasticity, our research examined only firing rate changes. The relationship between synaptic and firing rate regulations should be addressed in further studies. It is also worth considering that in our study we only measured from deep cortical layer neurons in frontal cortical regions of the rodent, which may not be fully representative neuronal dynamics in all cortical regions or in upper layers.

Activity-dependent firing rate regulation observed here during sleep is reminiscent of the dynamic restructuring of activity described during sensory deprivation (Margolis et al., 2012). When all whiskers but one were trimmed, stimulation of the spared whisker evoked diminished responses in the most active but enhanced responses in the least active somatosensory neurons. Activity of fast- and slow-firing neurons was also differentially affected in hippocampal neurons by sleep (Miyawaki and Diba, 2016). Overall, these findings suggest that differential regulation of slow- and fast-firing neurons is a cortex-wide phenomenon.

Our observations are also different from the prediction of the homeostatic scaling model (Turrigiano and Nelson, 2004). Instead of observing the firing rate distribution sliding to the left during sleep, we observed a decreased coefficient of population rate variation (Figure 6). Further research is needed to clarify the mechanisms responsible for the differential rate shifting and activity-centralizing homeostatic effects of sleep.

Overall, our findings imply that the various members of the lognormal firing rate distribution are affected by different mechanisms and that a rate-centralizing effect of sleep results from the parallel rate increase of slow-firing and decrease of fast-firing subpopulations. Redistribution of activity may be a mechanism by which learning-induced (cf. Rasch and Born, 2013) and homeostatic plastic processes can be balanced. We hypothesize that homeostatic downscaling affects mainly the minority high-firing neurons to provide network stability, whereas "silent" and slow-firing neurons comprise a large pool of reserve for learning, development, and regeneration-induced specific plasticity (Buzsáki and Mizuseki, 2014; Grosmark and Buzsáki, 2016; Margolis et al., 2012; Panas et al., 2015; Shoham et al., 2006).

Conclusions

We found that sleep does not simply decrease the overall firing rates of the population. Instead, multiple substates of sleep

exerted differential effects on neurons across the firing rate distribution during the cyclic course of sleep. In addition to the critical roles of nonREM and REM, our observations also point to the importance of MAs in sleep homeostasis to reduce firing rate dispersion. These global sleep processes might sustain a wide dynamic range of firing rates, both securing network stability via a sparse network of highly active neurons, and accommodating learning-induced changes via the flexible, slow-firing, plastic, neuronal majority.

EXPERIMENTAL PROCEDURES

Eleven male Long Evans rats, age 3–7 months, were implanted with 64-site silicon probes to record LFP and unit firing in the deep layers of frontal cortical areas (Vandecasteele et al., 2012). All recordings were carried out in the home cage of the animal during daytime hours. All protocols were approved by the Institutional Animal Care and Use Committee of New York University and Weill Cornell Medical College.

After separation of LFP and spike data, spikes were clustered into single units (Rossant et al., 2016) and separated into putative pyramidal cells and putative interneurons (Supplemental Experimental Procedures). Sleep scoring was performed by an automated algorithm and supervised manually, using LFP derivatives and EMG signals to segregate WAKE, nonREM, REM, and MA brain states. During nonREM, UP and DOWN states of slow oscillation were detected using spike and LFP criteria (Vyazovskiy et al., 2009), and sleep spindles after filtering and integration.

Putative single pyramidal neurons were divided into six subgroups (sextiles) based on their overall WAKE firing rates, and these same groups were applied across all analyses to ameliorate the possibility of "regression to the mean" effect (rather than regrouping prior to each analyzed epoch). Further details and discussion of the recordings and data analyses including spiking and LFP analyses are available in the Supplemental Experimental Procedures.

SUPPLEMENTAL INFORMATION

Supplemental Information includes Supplemental Experimental Procedures, five figures, and one table and can be found with this article online at http://dx.doi.org/10.1016/j.neuron.2016.03.036.

AUTHOR CONTRIBUTIONS

ACKNOWLEDGMENTS

REFERENCES

Avramescu, S., and Timofeev, I. (2008). Synaptic strength modulation after cortical trauma: a role in epileptogenesis. J. Neurosci. 28, 6760–6772.

Axmacher, N., Mormann, F., Fernández, G., Elger, C.E., and Fell, J. (2006). Memory formation by neuronal synchronization. Brain Res. Brain Res. Rev. 52, 170–182.

Bergmann, B.M., Winter, J.B., Rosenberg, R.S., and Rechtschaffen, A. (1987). NREM sleep with low-voltage EEG in the rat. Sleep 10, 1–11.

Besedovsky, L., Lange, T., and Born, J. (2012). Sleep and immune function. Pflugers Arch. 463, 121–137.

Bienenstock, E.L., Cooper, L.N., and Munro, P.W. (1982). Theory for the development of neuron selectivity: orientation specificity and binocular interaction in visual cortex. J. Neurosci. 2, 32–48.

Blanco, W., Pereira, C.M., Cota, V.R., Souza, A.C., Rennó-Costa, C., Santos, S., Dias, G., Guerreiro, A.M.G., Tort, A.B.L., Neto, A.D., and Ribeiro, S. (2015). Synaptic homeostasis and restructuring across the sleep-wake cycle. PLoS Comput. Biol. 11, e1004241.

Borbély, A.A. (1982). A two process model of sleep regulation. Hum. Neurobiol. 1, 195–204.

Brailowsky, S., Kunimoto, M., Silva-Barrat, C., Menini, C., and Naquet, R. (1990). Electroencephalographic study of the GABA-withdrawal syndrome in rats. Epilepsia 31, 369–377.

Buonomano, D.V. (2005). A learning rule for the emergence of stable dynamics and timing in recurrent networks. J. Neurophysiol. 94, 2275–2283.

Buzsáki, G. (2015). Hippocampal sharp wave-ripple: A cognitive biomarker for episodic memory and planning. Hippocampus 25, 1073–1188.

Buzsáki, G., and Mizuseki, K. (2014). The log-dynamic brain: how skewed distributions affect network operations. Nat. Rev. Neurosci. 15, 264–278.

Buzsáki, G., Bickford, R.G., Armstrong, D.M., Ponomareff, G., Chen, K.S., Ruiz, R., Thal, L.J., and Gage, F.H. (1988). Electric activity in the neocortex of freely moving young and aged rats. Neuroscience 26, 735–744.

Buzsáki, G., Csicsvari, J., Dragoi, G., Harris, K., Henze, D., and Hirase, H. (2002). Homeostatic maintenance of neuronal excitability by burst discharges in vivo. Cereb. Cortex 12, 893–899.

Calvet, J., Fourment, A., and Thiefry, M. (1973). Electrical activity in neocortical projection and association areas during slow wave sleep. Brain Res. 52, 173–187.

Campbell, I.G., and Feinberg, I. (1993). Dissociation of delta EEG amplitude and incidence in rat NREM sleep. Brain Res. Bull. 30, 143–147.

Cohen, S.M., Ma, H., Kuchibhotla, K.V., Watson, B.O., Buzsáki, G., Froemke, R.C., and Tsien, R.W. (2016). Excitation-transcription coupling in parvalbumin-positive interneurons employs a novel CaM Kinase-dependent pathway distinct from excitatory neurons. Neuron. S0896-6273(16)00180-X. Published online March 31, 2016. http://dx.doi.org/10.1016/j.neuron.2016.03.001.

Connors, B.W., and Gutnick, M.J. (1990). Intrinsic firing patterns of diverse neocortical neurons. Trends Neurosci. 13, 99–104.

Delgado, J.Y., Gómez-González, J.F., and Desai, N.S. (2010). Pyramidal neuron conductance state gates spike-timing-dependent plasticity. J. Neurosci. 30, 15713–15725.

Dijk, D.J., and Czeisler, C.A. (1995). Contribution of the circadian pacemaker and the sleep homeostat to sleep propensity, sleep structure, electroencephalographic slow waves, and sleep spindle activity in humans. J. Neurosci. 15, 3526–3538.

Douglas, N.J., and Martin, S.E. (1996). Arousals and the sleep apnea/hypopnea syndrome. Sleep 19 (10, Suppl), S196–S197.

Feinberg, I. (1974). Changes in sleep cycle patterns with age. J. Psychiatr. Res. 10, 283–306.

Frank, M.G., Issa, N.P., and Stryker, M.P. (2001). Sleep enhances plasticity in the developing visual cortex. Neuron 30, 275–287.

Gervasoni, D., Lin, S.-C., Ribeiro, S., Soares, E.S., Pantoja, J., and Nicolelis, M.A.L. (2004). Global forebrain dynamics predict rat behavioral states and their transitions. J. Neurosci. 24, 11137–11147.

Gierz, M., Campbell, S.S., and Gillin, J.C. (1987). Sleep disturbances in various nonaffective psychiatric disorders. Psychiatr. Clin. North Am. 10, 565–581.

Grosmark, A.D., and Buzsáki, G. (2016). Diversity in neural firing dynamics supports both rigid and learned hippocampal sequences. Science *351*, 1440–1443.

Grosmark, A.D., Mizuseki, K., Pastalkova, E., Diba, K., and Buzsáki, G. (2012). REM sleep reorganizes hippocampal excitability. Neuron *75*, 1001–1007.

Halász, P., Kundra, O., Rajna, P., Pál, I., and Vargha, M. (1979). Micro-arousals during nocturnal sleep. Acta Physiol. Acad. Sci. Hung. *54*, 1–12.

Ibata, K., Sun, Q., and Turrigiano, G.G. (2008). Rapid synaptic scaling induced by changes in postsynaptic firing. Neuron *57*, 819–826.

Inostroza, M., and Born, J. (2013). Sleep for preserving and transforming episodic memory. Annu. Rev. Neurosci. *36*, 79–102.

Kim, J., and Tsien, R.W. (2008). Synapse-specific adaptations to inactivity in hippocampal circuits achieve homeostatic gain control while dampening network reverberation. Neuron *58*, 925–937.

Lim, S., McKee, J.L., Woloszyn, L., Amit, Y., Freedman, D.J., Sheinberg, D.L., and Brunel, N. (2015). Inferring learning rules from distributions of firing rates in cortical neurons. Nat. Neurosci. *18*, 1804–1810.

Luczak, A., Barthó, P., Marguet, S.L., Buzsáki, G., and Harris, K.D. (2007). Sequential structure of neocortical spontaneous activity in vivo. Proc. Natl. Acad. Sci. USA *104*, 347–352.

Luczak, A., McNaughton, B.L., and Harris, K.D. (2015). Packet-based communication in the cortex. Nat. Rev. Neurosci. *16*, 745–755.

Margolis, D.J., Lütcke, H., Schulz, K., Haiss, F., Weber, B., Kügler, S., Hasan, M.T., and Helmchen, F. (2012). Reorganization of cortical population activity imaged throughout long-term sensory deprivation. Nat. Neurosci. *15*, 1539–1546.

Markram, H., Lübke, J., Frotscher, M., and Sakmann, B. (1997). Regulation of synaptic efficacy by coincidence of postsynaptic APs and EPSPs. Science *275*, 213–215.

McCarley, R.W. (2007). Neurobiology of REM and NREM sleep. Sleep Med. *8*, 302–330.

Miller, K.D. (1996). Synaptic economics: competition and cooperation in synaptic plasticity. Neuron *17*, 371–374.

Mitra, A., Mitra, S.S., and Tsien, R.W. (2012). Heterogeneous reallocation of presynaptic efficacy in recurrent excitatory circuits adapting to inactivity. Nat. Neurosci. *15*, 250–257.

Miyawaki, H., and Diba, K. (2016). Regulation of hippocampal firing by network oscillations during sleep. Curr. Biol. *26*, 893–902.

Mizuseki, K., and Buzsáki, G. (2013). Preconfigured, skewed distribution of firing rates in the hippocampus and entorhinal cortex. Cell Rep. *4*, 1010–1021.

Panas, D., Amin, H., Maccione, A., Muthmann, O., van Rossum, M., Berdondini, L., and Hennig, M.H. (2015). Sloppiness in spontaneously active neuronal networks. J. Neurosci. *35*, 8480–8492.

Peyrache, A., Benchenane, K., Khamassi, M., Wiener, S.I., and Battaglia, F.P. (2010). Sequential reinstatement of neocortical activity during slow oscillations depends on cells' global activity. Front. Syst. Neurosci. *3*, 18.

Pickenhain, L., and Klingberg, F. (1967). Hippocampal slow wave activity as a correlate of basic behavioral mechanisms in the rat. Prog. Brain Res. *27*, 218–227.

Rabinowitch, I., and Segev, I. (2008). Two opposing plasticity mechanisms pulling a single synapse. Trends Neurosci. *31*, 377–383.

Rasch, B., and Born, J. (2013). About sleep's role in memory. Physiol. Rev. *93*, 681–766.

Rossant, C., Kadir, S.N., Goodman, D.F., Schulman, J., Hunter, M.L., Saleem, A.B., Grosmark, A., Belluscio, M., Denfield, G.H., Ecker, A.S., et al. (2016). Spike sorting for large, dense electrode arrays. Nat. Neurosci *19*, 634–641.

Rutherford, L.C., Nelson, S.B., and Turrigiano, G.G. (1998). BDNF has opposite effects on the quantal amplitude of pyramidal neuron and interneuron excitatory synapses. Neuron *21*, 521–530.

Schieber, J.P., Muzet, A., and Ferriere, P.J. (1971). [Phases of spontaneous transitory activation during normal sleep in humans]. Arch. Sci. Physiol. (Paris) *25*, 443–465.

Schmitzer-Torbert, N., Jackson, J., Henze, D., Harris, K., and Redish, A.D. (2005). Quantitative measures of cluster quality for use in extracellular recordings. Neuroscience *131*, 1–11.

Sejnowski, T.J., and Destexhe, A. (2000). Why do we sleep? Brain Res. *886*, 208–223.

Shoham, S., O'Connor, D.H., and Segev, R. (2006). How silent is the brain: is there a "dark matter" problem in neuroscience? J. Comp. Physiol. A Neuroethol. Sens. Neural Behav. Physiol. *192*, 777–784.

Siccoli, M.M., Rölli-Baumeler, N., Achermann, P., and Bassetti, C.L. (2008). Correlation between sleep and cognitive functions after hemispheric ischaemic stroke. Eur. J. Neurol. *15*, 565–572.

Stellwagen, D., and Malenka, R.C. (2006). Synaptic scaling mediated by glial TNF-alpha. Nature *440*, 1054–1059.

Stepanski, E., Lamphere, J., Badia, P., Zorick, F., and Roth, T. (1984). Sleep fragmentation and daytime sleepiness. Sleep *7*, 18–26.

Steriade, M. (2006). Grouping of brain rhythms in corticothalamic systems. Neuroscience *137*, 1087–1106.

Steriade, M., McCormick, D.A., and Sejnowski, T.J. (1993). Thalamocortical oscillations in the sleeping and aroused brain. Science *262*, 679–685.

Steriade, M., Timofeev, I., and Grenier, F. (2001). Natural waking and sleep states: a view from inside neocortical neurons. J. Neurophysiol. *85*, 1969–1985.

Stickgold, R., Whidbee, D., Schirmer, B., Patel, V., and Hobson, J.A. (2000). Visual discrimination task improvement: A multi-step process occurring during sleep. J. Cogn. Neurosci. *12*, 246–254.

Thiagarajan, T.C., Lindskog, M., and Tsien, R.W. (2005). Adaptation to synaptic inactivity in hippocampal neurons. Neuron *47*, 725–737.

Tononi, G., and Cirelli, C. (2003). Sleep and synaptic homeostasis: a hypothesis. Brain Res. Bull. *62*, 143–150.

Tononi, G., and Cirelli, C. (2014). Sleep and the price of plasticity: from synaptic and cellular homeostasis to memory consolidation and integration. Neuron *81*, 12–34.

Trachsel, L., Tobler, I., and Borbély, A.A. (1988). Electroencephalogram analysis of non-rapid eye movement sleep in rats. Am. J. Physiol. *255*, R27–R37.

Turrigiano, G.G., and Nelson, S.B. (2004). Homeostatic plasticity in the developing nervous system. Nat. Rev. Neurosci. *5*, 97–107.

Turrigiano, G.G., Leslie, K.R., Desai, N.S., Rutherford, L.C., and Nelson, S.B. (1998). Activity-dependent scaling of quantal amplitude in neocortical neurons. Nature *391*, 892–896.

Vandecasteele, M., M, S., Royer, S., Belluscio, M., Berényi, A., Diba, K., Fujisawa, S., Grosmark, A., Mao, D., Mizuseki, K., et al. (2012). Large-scale recording of neurons by movable silicon probes in behaving rodents. J. Vis. Exp. (61), e3568, http://dx.doi.org/10.3791/3568.

Vyazovskiy, V.V., and Harris, K.D. (2013). Sleep and the single neuron: the role of global slow oscillations in individual cell rest. Nat. Rev. Neurosci. *14*, 443–451.

Vyazovskiy, V.V., Riedner, B.A., Cirelli, C., and Tononi, G. (2007). Sleep homeostasis and cortical synchronization: II. A local field potential study of sleep slow waves in the rat. Sleep *30*, 1631–1642.

Vyazovskiy, V.V., Olcese, U., Lazimy, Y.M., Faraguna, U., Esser, S.K., Williams, J.C., Cirelli, C., and Tononi, G. (2009). Cortical firing and sleep homeostasis. Neuron *63*, 865–878.

Walker, M.P. (2010). Sleep, memory and emotion. Prog. Brain Res. *185*, 49–68.

Wilson, C.J., and Groves, P.M. (1981). Spontaneous firing patterns of identified spiny neurons in the rat neostriatum. Brain Res. *220*, 67–80.

Xie, L., Kang, H., Xu, Q., Chen, M.J., Liao, Y., Thiyagarajan, M., O'Donnell, J., Christensen, D.J., Nicholson, C., Iliff, J.J., et al. (2013). Sleep drives metabolite clearance from the adult brain. Science *342*, 373–377.